Wiley
Structural Control and Health Monitoring
Volume 2024, Article ID 2865576, 16 pages
https://doi.org/10.1155/2024/2865576

WILEY

Research Article

Economic Impact Assessment of Structural Health Monitoring Systems on Helicopter Blade Beginning of Life

Pietro Ballarin,[1] **Marco Macchi**,[2] **Irene Roda**,[2] **Giuseppe Sala**,[1] **Andrea Baldi**,[3] **and Alessandro Airoldi**[1]

[1]*Department of Aerospace Science and Technology, Politecnico di Milano, Via La Masa 34, Milan 20156, Italy*
[2]*Department of Management, Economics, and Industrial Engineering, Politecnico di Milano, Via Lambruschini 4/B, Milan 20156, Italy*
[3]*Leonardo S.p.A., Helicopters Division, Via Giovanni Agusta 520, Cascina Costa di Samarate 21017, Italy*

Correspondence should be addressed to Pietro Ballarin; pietro.ballarin@polimi.it

Received 15 April 2024; Revised 6 August 2024; Accepted 21 August 2024

Academic Editor: Hoon Sohn

The economic impact of Structural Health Monitoring Systems based on optical fibre sensors is assessed in the development of composite helicopter rotor blades. Hence, the focus of this analysis is on the helicopter's Beginning Of Life stage. Two applications of the Structural Health Monitoring System are considered in the development of composite blades: curing cycle development and accomplishment of laboratory and flight certification tests. Optical fibre sensors measure the temperature field during the curing cycle and strain field during the laboratory tests and allow load identification during the load survey activity. It was found that Structural Health Monitoring Systems can potentially lead to economic benefits during the development of the blade provide that a reduction in the number of curing cycles and number of blades tested is achieved as a consequence of the improvement of the temperature and strain field quality. Moreover, an economic benefit could be achieved during the load survey activity, needed to complete the certification of the composite blade, avoiding the periodical maintenance of the applied strain gauges acquiring the strains during the flight.

1. Introduction

Safety represents a fundamental characteristic in the aeronautical field. Indeed, it is vital to avoid safety loss due to a failure of a structure, which could potentially lead to the loss of the aircraft and human lives. In order to guarantee an adequate safety level, aeronautical structures are subjected to a maintenance program [1–3], whose associate costs are not negligible and can reach up to over 27% of the total lifecycle cost of a fixed-wing aircraft [4]. For metallic aeronautical structures, inspection plans are established considering a damage growth approach, for which a damage with a predefined size is supposed to grow under fatigue loads that are expected during the operational life of the aircraft [5]. For composite structures, the inspection plans are defined considering a no-grow approach and assuming that during the operational life, some damages will occur and, in that timeframe, the applied loads may exceed the residual strength of the structure [6]. However, the real load spectra encountered during the operational life could be different with respect to the one applied to the structure during the tests, as well as some damages can be missed during the inspection of the structure: all these aspects contribute to increase the level of uncertainty about the structural integrity of the aircraft. Currently, aerospace structures are subjected to different levels of inspection, starting from the General Visual Inspection (GVI) to the Detailed Inspection (DI). In the latter, different types of nondestructive Techniques (NDT) are employed in order to inspect the structure [7]. Radiography is commonly adopted for composite components [8] as well as ultrasounds are widely diffused [9]. Despite the effectiveness of such techniques, their usage results to be expensive since they require the operator manpower and the aircraft on ground, so reducing the fleet

availability. The possibility to have a continuous monitoring of the structure can be provided by the Structural Health Monitoring Systems (SHMS). Their application to aerospace structures was widely investigated in the last 20 years [10–12]. Different types of SHMS were presented, like piezoelectric, comparative vacuum, and optical fibre-based (OF-based). Among all of them, OF-based SHMS [13–15] seems to be the most promising because of their low weight, low required volume, low sensitivity to electromagnetic disturbances, and the possibility to be embedded and protected inside the composite laminates [16]. Besides, composite materials are widely adopted to build aeronautical structures; this is enabling a large possibility to apply OF-based SHMS. Despite the high level of development and potential of such systems, their application in the industrial field is still not diffused: there are several reasons for that, one of them is the potential panic that a false alarm may cause during the flight, and another reason relies in the lack of methods aimed at evaluating their impact from an economic point of view. In the literature, some studies were carried out to assess the economic impact of SHMS [4, 17–21], but most of them are applied to conventional metallic structures related to aircraft and considering other types of SHMS out of the OF-based. Moreover, all of them focus on the usage phase of the aircraft, not considering the impact that the Original Equipment Manufacturer (OEM) could gain. Indeed, the economic impact of SHMS can be analysed considering the lifecycle of the aircraft, looking both at the Middle Of Life (MOL) and Beginning Of Life (BOL) phases. Focusing on the MOL phase means analysing the effects that the SHMS has on the operational life of the machine; this includes the effect on the maintenance of the aircraft, on the consumed fuel and fleet availability. Focusing on the BOL phase means analysing the effects that the SHMS has on the production and delivery stage of the aircraft, which may include its development and certification. The objective of this paper is to investigate this aspect and to develop a supporting tool aimed at quantitatively evaluating the impact of OF-based SHMS on the BOL of composite helicopter rotor blades. Some studies were presented in the literature regarding the automatic identification of the structural dynamics of helicopter blades [22, 23], including the usage of OF [24], with the potential to identify the presence of damages observing the outliers; however, the economic impact of SHMS was not investigated in the literature for such kind of structural elements. Currently, there are only few studies regarding the impact of SHMS on the MOL phase [4, 17–21] and, to the best of authors' knowledge, no one regarding the BOL. Moreover, it is worth remarking that detailed Life Cycle Costing (LCC) standards are related to other application cases, such as the case of *Oil&Gas* [25–27]. The model developed in this work aims at performing a comparative analysis between the current state in which blades are produced without SHMS, hereinafter named as "as is" scenario, and the one including the SHMS, hereinafter named as scenario "with SHMS." The LCC methodology [28] is exploited, building the BOL perspective.

This paper is organized as it follows. In section 2, a description of the scenarios is given; therein, it is described the role of the SHMS and the potential benefits that they are expected to provide. In section 3, the scenarios are modelled using the IDEF0 methodology in order to make explicit the contributions and impacts on processes within the BOL perspective; in the light of the IDEF0 formalization, the cost model is consistently derived. In section 4, an implementation of the cost model is discussed, together with some sensitivity analyses enabling to quantify the effects of the variation of some parameters. Finally, in section 5, conclusions, results, and main findings are given.

2. SHMS Application Scenarios

SHMS were widely investigated in terms of their application to monitor the aircraft structures during their operational life, but rarely their impact on the production stage was studied. In this work, an experimental case is investigated considering a composite helicopter tail rotor blade, which is supposed to be sensorized with Fibre Bragg Grating (FBG) sensors inscribed inside the OF. Although the potential advantages provided by the FBG sensors, they show two main drawbacks: cost of sensors and integration in the host material. Indeed, the cost of 1 FBG sensor can reach up to 100 €, and considering the high density of FBG sensors required to monitor the state of integrity of a structure, this leads to significantly increase the cost of the sensorized structure. The problem of sensors integration was extensively investigated in [15, 16, 29]. One of the problems is represented by the connection of the OF with the external environment, which is needed to acquire the strain signals during the operational life. This issue is often addressed using polymeric additive manufactured connectors, either positioned on the surface of the laminate [30] or embedded inside the laminate [29]. The lamination sequence also has an influence on the strain reading performance of the FBG sensors, and particular care must be taken to align the OF axis with the reinforcement fibers of the laminate to avoid the microbending of the OF, which can affect the transmitted signal.

Two application scenarios of the SHMS are considered: the former is related to the laboratory activities necessary to develop the blade, including a first stage of its certification, and the latter is related to the employment of the FBG sensors during the load survey activity, in which the component is equipped with strain gauges and mounted on helicopter prototypes performing different flight manoeuvres as request by the design usage spectrum. Such activity allows completing the certification of the component.

2.1. Description of Beginning of Life. The lifecycle of most of the products can be divided into three phases, BOL, MOL, and End Of Life (EOL) [31–33], the latter is related to the disposal phase of the product. MOL is focused on the usage phase of the product, once the aircraft or a helicopter, delivered to the customer, is employed to perform all the tasks needed, such as passengers (PAX) or goods (Utility) transportation, Offshore (OFF), as well as Search And Rescue (SAR). BOL represents the life of the product

included between the production and its delivery to the market and to the customer.

Considering the product as the composite helicopter tail rotor blade, the BOL phase can be divided into three main steps:

(i) The first step to face when a new composite component needs to be produced is to find the right technological processes ensuring a satisfactory quality. For example, a proper lamination technique must be set up so to reduce as minimum as possible material scrap, ensuring a proper fibre alignment, avoiding wrinkling and the creation of voids. Another important aspect is related to the definition of the autoclave curing cycle, which is needed to polymerize the composite prepreg material. In fact, depending on the geometry and the material of the component, a specific distribution of the temperature over time needs to be applied in order to guarantee a uniformly temperature distribution inside the component.

(ii) The second step is related to the first stage of component's certification, which consists in the execution of laboratory tests. The OEM must perform some mechanical tests aimed at demonstrating to the certification authorities (for example, EASA for Europe and FAA for USA) that the component withstands the ultimate and fatigue loads, as well as resistance to impacts and ageing. Certification tests regarding the effects of possible technological defects are also required.

(iii) The third step is related to the second stage of component's certification, which consists in the execution of a load survey activity. In this phase, the component is equipped with strain gauges and subsequently mounted on helicopter prototypes; during the flight, different manoeuvres are performed and the strains provided by the strain gauges are acquired. A damage accumulation parameter is computed and the fatigue life of the component is estimated. This stage represents the end of the certification process of the component. Eventually, an additional load survey activity may be performed to extend the flight envelope of the helicopter to a wider range.

The three steps are considered in this work as the fundamentals to provide the process description of the BOL of the blade. The next subsections within this section 2 illustrate the scenarios with more details: the first and second steps determine the laboratory activities (subsection 2.2), while the third step pertains to the load survey activity (subsection 2.3). Section 3 will provide a further formalization of the process with the IDEF0 methodology.

2.2. SHMS Application to Laboratory Activities. A first application of the FBG sensors was found in the support to the composite tail rotor blade laboratory activities needed for its development. In fact, when a new composite component is produced, the production cycle – including the lamination process and the curing cycle – needs to be carefully engineered. Then, the certification process should be performed.

Considering the curing cycle, as it is already known the crosslinking reaction of composite thermoset material is exothermic, this represents one of the reasons for the discrepancy between the temperature imposed through the autoclave cycle and the real one [34]. This aspect can also create problems related to the generation of thermal residual stresses [35] inside the material. Nowadays, the monitoring of the temperature inside the material is obtained by embedding thermocouples inside the component at different locations. Being aware of the equivalence in the temperature reading of FBG sensors and thermocouples, as it was demonstrated in [35], a possible application of the FBG sensors would be to embed them inside the material with the aim to monitor the temperature during the curing cycle, as it is already presented in the literature [35–37]. The high number of FBG sensors needed to monitor the component could be exploited to monitor also the temperature distribution in a higher number of locations and with a better accuracy with respect to what performed using thermocouple. A benefit is then expected as a consequence of this characteristic: a lower number of blades would be necessary to find the proper curing cycle. In Figure 1, the manufacturing process of a sensorized composite tail rotor blade is shown.

Once the curing cycle is established, the first stage of the certification process must be faced and laboratory mechanical tests need to be performed. Currently, this is done applying strain gauges at different locations on the component and subsequently testing the blade in different load conditions. Moreover, laboratory tests require including artificially induced defects in order to evaluate their propagation under fatigue loads and to evaluate their effects on the residual strength. Such tests are time-consuming, especially the fatigue ones, and they require a lot of resources. For example, some problems may arise in reading the strain values from the strain gauges, especially when artificial defects are introduced. This aspect impacts the time and resource consumption as it requires further verifications and in the worst case, the production of another blade for testing. As another problem, strain gauges are subjected to wear due to contact oxidation; this also impacts the time and resource consumption as it may require the accomplishment of a new test and/or a new strain gauge application on the blade. Since the equivalence in the strain reading performance of strain gauges and FBG sensors was demonstrated in [39], the presence of the SHMS can be exploited by acquiring from the FBG sensors the information about the strain field, so avoiding applying multiple times the strain gauges on the blade. The presence of such sensors could also potentially lead to a higher accuracy of the strain data read during the test, so avoiding its repetition induced by a low data quality. Eventually, FBG sensors may also monitor temperature during the test execution, thus accounting for temperature effects to the strain field and further improving the accuracy of the acquired data. Figure 2 shows the blade root subjected

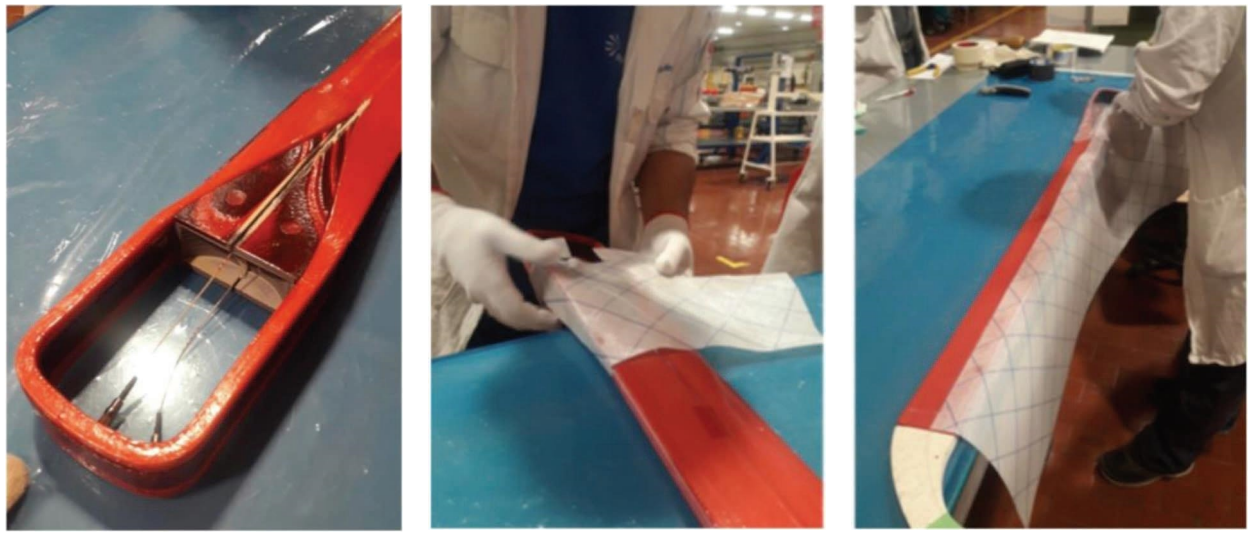

(a) (b) (c)

Figure 1: Manufacturing process of a composite tail rotor blade. (a) Detail regarding the optical fibres; (b) and (c) detail regarding the application of the antitorsional layer. Adapted from [38] with permission of the authors.

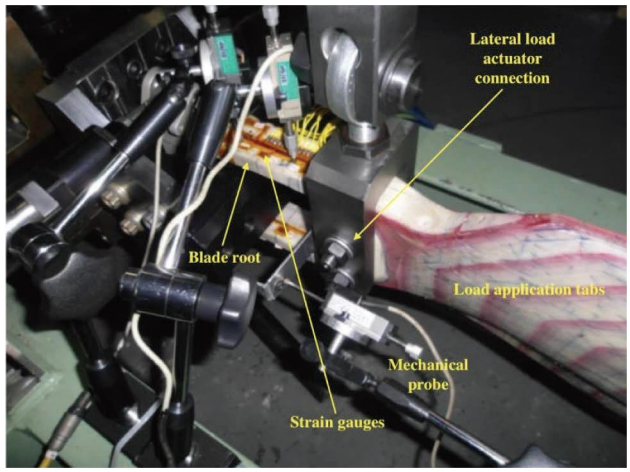

Figure 2: Blade root subjected to laboratory tests needed to complete the first stage of the certification.

to mechanical laboratory tests, in which the component is loaded in a test rig.

2.3. SHMS Application to Load Survey Activity. The second application is represented by the usage of the SHMS to support the load survey activity. The objective is to analyse flight data and to acquire a more detailed load spectrum acting on the helicopter's component. To do this, the OEM must equip some helicopter prototypes with accelerometers and strain gauges that, during the flight, will provide the desired information. This task of course requires the technicians to apply strain gauges and accelerometers on the helicopter's structure, leading to the generation of costs especially related to manpower. The application of the SHMS fits in this scenario considering the helicopter blades already produced with SHMS assembled on the helicopter: in this case, the main advantage is that the blade does not need to be equipped with strain gauges. Moreover, strain gauges are subjected to wear, due for example to contact oxidation or disbonding, which would be avoided using FBG sensors. Load survey activity represents the last stage of the certification process of the component; however, considering a component already certified, another load survey activity may be carried out with the aim to extend the flight envelope of the helicopter. Also, in this case, the component sensorized with FBG sensors can avoid the application of the strain gauges, reducing the required manpower.

3. Cost Model Definition

In order to define the cost model, as Cost Breakdown Structure (CBS), it is necessary to map the activities and put in evidence their *inputs* and *outputs* together with the *resources* consumed to perform the activities and the *controls* imposed, up to finally identifying the cost elements in the CBS. The IDEF0 is used to this end, thus finally enabling to map the process across the application scenarios presented in section 2. Indeed, the objective of this work is to provide a cost model aimed at evaluating the economic impact related to the usage of SHMS on a composite rotor blade compared with the current situation, represented by the scenario "as is." Only the cost elements that are differential between the scenarios are modelled, while the cost elements common to both the scenarios are neglected. To support the comparison of the two scenarios designated as "as is" and "with SHMS," the IDEF0 diagrams adopted the following colour code conventions:

(i) Red colour, related to activity/resources/inputs/controls specific to the "as is" scenario, without the usage of SHMS;

(ii) Green colour, related to the activity/resources/inputs/controls specific to the scenario "with SHMS";

(iii) Black colour, related to the activity/resources/inputs/controls common to both the scenarios.

Building on the activity/resources/inputs/controls depicted in the IDEF0 formalization, the cost elements can be derived as mathematical expressions of the consumed time and resources.

3.1. Laboratory Activities. In Figure 3, the IDEF0 diagram related to the laboratory activities can be observed with its three macro-activities, namely, *train workers* (marked as A1), *develop curing cycle* (marked as A2), and *perform laboratory tests* (marked as A3). A1 macro-activity is related to the training of the workers, which is needed to perform their task, such as laminate the composite blade or perform quality checks. A2 macro-activity is related to the development of the curing cycle, whose objective is to find the proper autoclave temperature distribution over time in order to obtain the desired mechanical properties while limiting the presence of residual thermal stresses. A3 macro-activity is related to the execution of laboratory tests, in fact, once the proper curing cycle is found, the mechanical properties of the blade need to be assessed: this is done performing static and fatigue tests on the blade subjected to different load conditions and introducing artificial defects to evaluate the residual strength.

Since for macro-activity A1, no subactivities are considered, Figure 4 shows the details of the macro-activity A2 in which all the subactivities are depicted. The only input is represented by the material to produce the blade, here named as prepreg. The macro activity has two outputs: blade scrap and curing cycle. The former is due to a faulty curing before finding the proper curing cycle, and the other is represented by the curing cycle itself. According to the "as is" scenario, the mould hosting the blade is cleaned and prepared with releasing agents and the blade is laminated using prepreg plies (activity A2-1) and thermocouples are then embedded in the laminate (activity A2-3). A vacuum bag is prepared, and the laminate is polymerized and removed from the mould (activity A2-4). After the polymerization, the data acquired by the thermocouples are analysed in order to identify the material temperature during the curing cycle and this operation is repeated until the desired material temperature is reached by acting on the curing cycle parameters (activities A2-5 and A2-6). The blade is also analysed after the polymerization using destructive and nondestructive controls (activities from A2-9 to A2-12). Destructive controls require the cutting of the blade in order to inspect visually the internal part of the component, typically using microscopes. Nondestructive controls instead consist in performing a radiography. Once both destructive and nondestructive controls meet the requirements and the temperature read by the thermocouples is the one desired, and the curing cycle can be established (activity A2-13).

Considering the scenario "with SHMS" during the lamination process (performed in activity A2-1), the FBG sensors are embedded inside the laminate (activity A2-2). During the polymerization (performed in activity A2-4), their signal is acquired and analysed to evaluate the temperature (activities A2-7 and A2-8), similarly to what is done with thermocouples. As it was done in the "as is" scenario, destructive and nondestructive controls are performed (activities from A2-9 to A2-12), and once all the requirements are met, the curing cycle is defined (activity A2-13). The expected advantage using FBG sensors is that their high number, combined with their low invasiveness and immunity to electromagnetic disturbances, will increase the accuracy of the temperature field. Consequently, the expected benefit is that a lower number of curing cycle repetitions is necessary to define the right one.

Figure 5 shows the subactivities related to the macro-activity A3 and represents the tests performed in the laboratory. The input of the process is the composite material prepreg, and the scraped blades and the first stage of blade certification represent the outputs.

Considering the "as is" scenario, the first stage concerns the production of the blade, so the mould is prepared and plies are stacked (activity A3-1), and subsequently, thermocouples are applied to the mould (activity A3-3): this activity is slightly different compared to the embedment of thermocouples during the development of the curing cycle (activity A2-3) since here thermocouples are applied over the mould; nevertheless, the corresponding time needed was considered to be the same. Once the thermocouples are applied to the mould, the vacuum bag is prepared and the blade is polymerized and removed from the mould (activity A3-4) adopting the curing cycle in output from macro-activity A2. Temperatures are checked during the polymerization (activity A3-5), and then the blade is equipped with strain gauges (activity A3-7) and subsequently tested (activity A3-8). During testing, the strain gauge signals are acquired (activity A3-9) and evaluated (activity A3-10): if they meet the requirements, the first stage of blade certification is completed (activity A3-13). It must be highlighted that strain monitoring with strain gauges may be particularly critical as they may not be glued properly to the surface of the component or their signal can be affected by electromagnetic disturbances. For such a reason, it could happen that some tests on the blade must be repeated, thus leading to the production of a new blade.

Considering the scenario "with SHMS," the blade is produced introducing the FBG sensors (activity A3-2) in the lamination phase (activity A3-1). During the curing phase (activity A3-4), the information about temperature is acquired by the FBG sensors (activity A3-6). Differently from the "as is" scenario, in this case, there is no need to equip the blade with strain gauges. Being the FBG sensors embedded in the component, they can be used to acquire (activity A3-11) the strain during the test phase (activity A3-12). If the test data meet the requirements, the first stage of blade certification is completed. In this case, the possible advantages from using SHMS can be the following twos: first, there is no need to equip the blade with strain gauges, and second, the monitoring of the blade with FBG sensors could provide more accurate information about the strain field of the component, thus leading to a possible reduction in the number of blades to be tested.

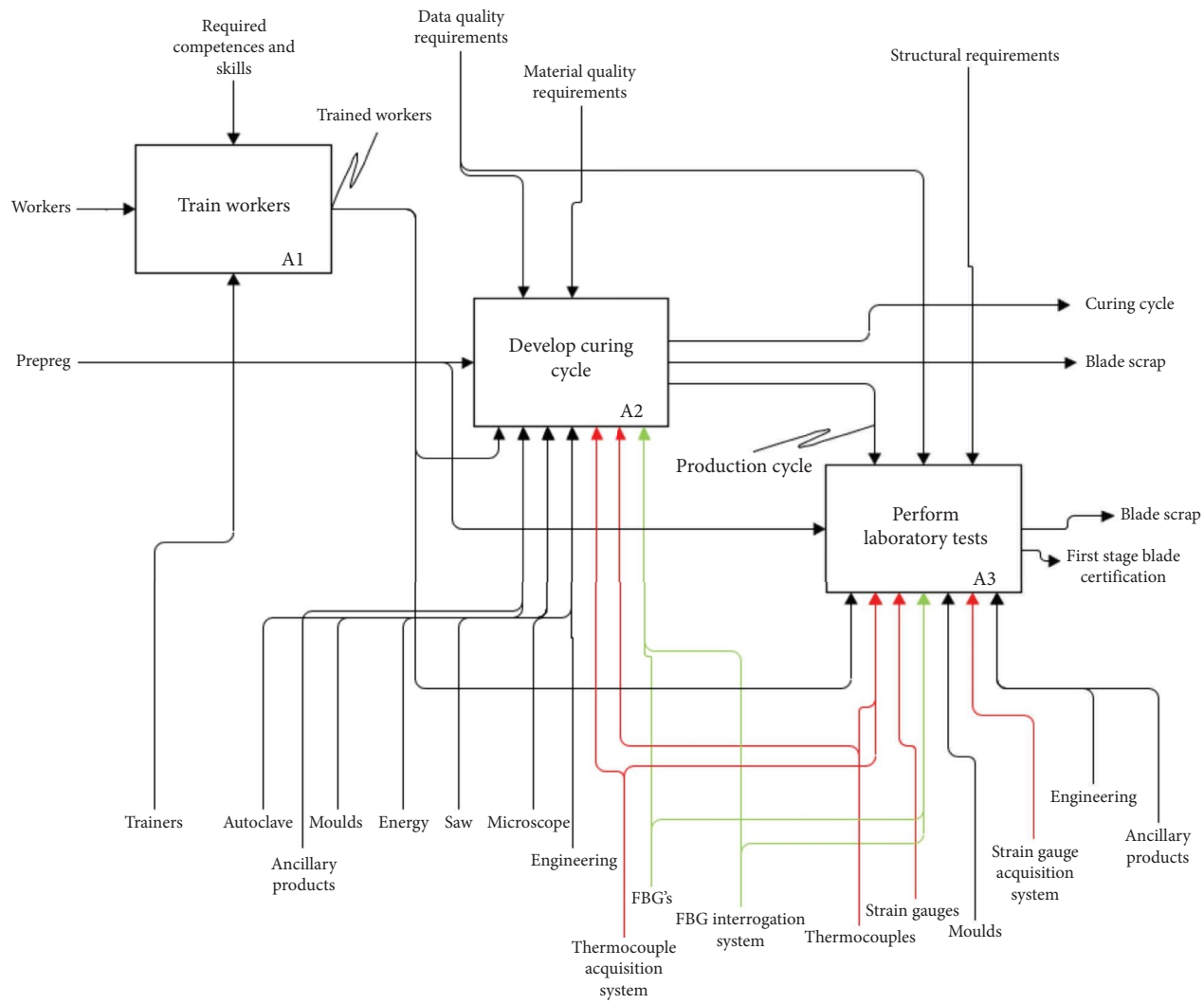

FIGURE 3: Laboratory activities modelled with IDEF0 formalism.

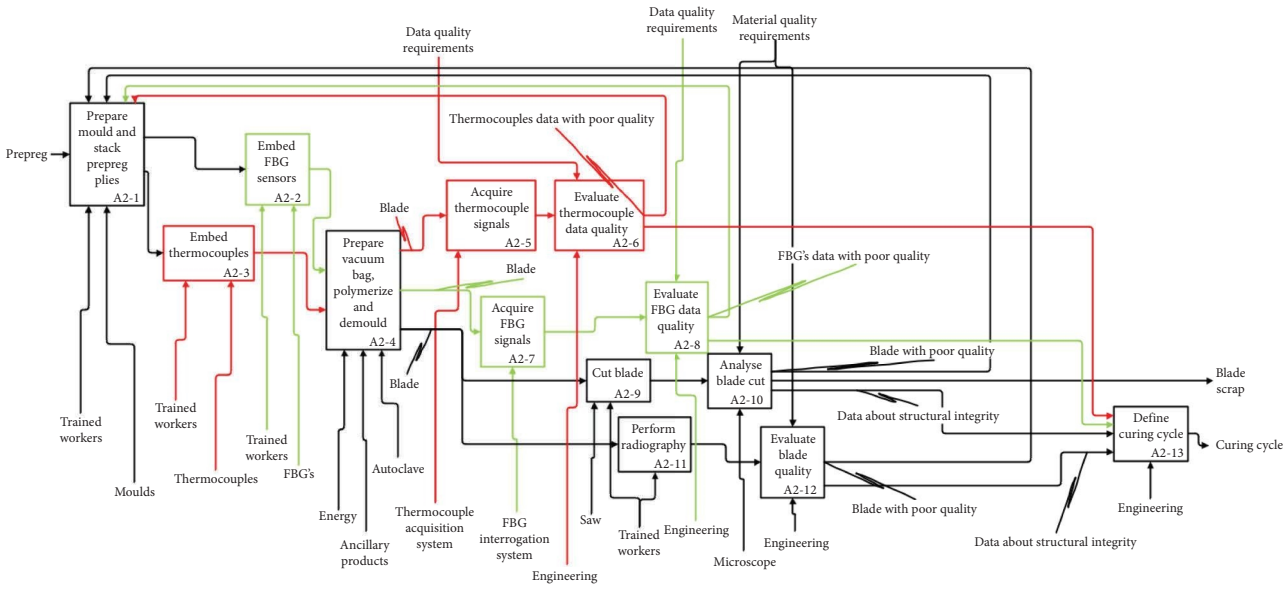

FIGURE 4: Activity A2, detail regarding the development of the curing cycle modelled with the IDEF0 formalism.

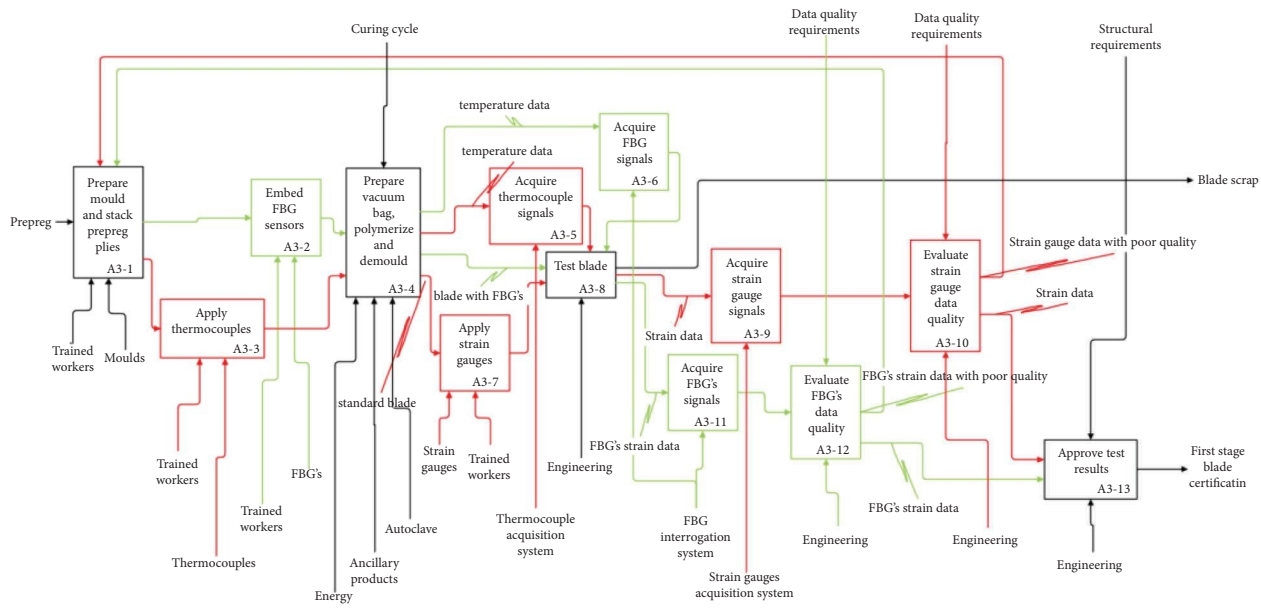

FIGURE 5: Activity A3, detail regarding the execution of laboratory tests modelled with IDEF0 formalism.

The cost model related to the laboratory activities is subsequently defined. Remarking that it expresses a differential cost between the two scenarios, the cost model is represented by equation (1).

$$C_{\text{lab act}} = C_{\text{cur cycle def}} + C_{\text{test lab}}. \tag{1}$$

As it can be observed, the cost model can be split into two parts, coherently with the process: one is related to the definition of the production (curing) cycle and the other is related to the cost of the tests needed to complete the first stage of blade certification. It is assumed that the same acquisition system for the scenarios "as is" is used for both the measurement of temperature data with thermocouples and for the measurements of the strain gauges during the certification tests. The same assumption is made for the FBG interrogation system in the scenario "with SHMS": the same interrogator is used to acquire temperature data during curing and strain data during tests for certification. The cost related to the development of the curing cycle is detailed in equation (2), considering the "as is" scenario.

$$C^{\text{as is}}_{\text{cur cycle def}} = \left(C_m m_{\text{blade}} + L_{\text{tr wo}}\left(t_{\text{lam}} + t_{em\,th} n_{th} + t_{\text{bag}} + t_{\text{mould}} + t_{\text{demould}}\right) + n_{th} C_{th} + C_{\text{en}} t_{\text{auto}} + t_{ev\,th} L_{\text{eng}}\right) n^{\text{as is}}_{\text{auto}} + C_{\text{th sys}}. \tag{2}$$

Thermocouples are assumed to be scraped at each curing cycle, and such hypothesis is justified since in this phase, they are fully embedded inside the component and cannot be used for further curing cycles. The cost of ancillary products like vacuum bag and tacky tape was supposed to be negligible, especially if compared with the cost related to the lamination time. The term $C_{\text{th sys}}$ represents the cost of the acquisition system attributed to the activity of curing cycle development. Since it is supposed to perform both the activities of temperature and strain monitoring, a cost partition was performed in relation to the time needed for each of these two activities according to equation (3):

$$C_{\text{th sys}} = C_{\text{acq sys}} \frac{t_{\text{auto}} n^{\text{as is}}_{\text{auto}}}{t_{\text{auto}} n^{\text{as is}}_{\text{auto}} + t_{\text{t b}} n^{\text{as is}}_{\text{test}}}. \tag{3}$$

Equation (4) represents the cost model related to the tests needed for the first stage of blade certification in laboratory in the "as is" scenario.

$$\begin{aligned} C^{\text{as is}}_{\text{test lab}} = &\left(C_m m_{\text{blade}} + L_{tr\,wo}\left(t_{lam} + t_{em\,th} n_{th} + t_{\text{bag}} + t_{\text{mould}} + t_{\text{demould}} + t_g n_g\right)\right. \\ &\left. + C_{en} t_{\text{auto}} + C_g n_g + L_{\text{eng}}\left(t_{t\,b} + t_{ev\,g}\right)\right) n^{\text{as is}}_{\text{test}} + C_{th} n_{th} + C_{\text{test sys}}. \end{aligned} \tag{4}$$

In this case, thermocouples are assumed to be used across different curing cycles, such hypothesis is justified since in this phase, they are applied on the mould and so can be reused for more cycles. $C_{\text{test sys}}$ represents the cost of the acquisition system used to read strain signal with strain gauges attributed to the activity of blade testing in the laboratory; it is calculated according to equation (5) and following the same cost partitioning principle adopted for equation (3).

$$C_{\text{test sys}} = C_{\text{acq sys}} \frac{t_{tb} n_{\text{test}}^{\text{as is}}}{t_{auto} n_{\text{auto}}^{\text{as is}} + t_{tb} n_{\text{test}}^{\text{as is}}}. \tag{5}$$

The cost model related to the development of the curing cycle considering the scenario "with SHMS" is represented in equation (6).

$$\begin{aligned} C_{\text{cur cycle def}}^{\text{SHMS}} = &\left(C_m m_{\text{blade}} + L_{tr\,wo}\left(t_{lam} + t_{em\,FBG} n_{FBG} + t_{\text{bag}} + t_{\text{mould}} + t_{\text{demould}}\right)\right. \\ &\left. + C_{FBG} n_{FBG} + C_{en} t_{\text{auto}} + L_{\text{eng}} t_{ev\,FBG}\right) n_{\text{auto}}^{\text{SHMS}} + C_{\text{th FBG sys}}, \end{aligned} \tag{6}$$

where $C_{\text{th FBG sys}}$ represents the cost of the FBG interrogation system attributed to the activity of curing cycle development. Similarly to the cost partitioning adopted in equation (3), the interrogation system is supposed to perform the activities of temperature and strain monitoring, so the cost attributed to the development of the curing cycle was calculated according to equation (7):

$$C_{\text{th FBG sys}} = C_{\text{FBG sys}} \frac{t_{\text{auto}} n_{\text{auto}}^{\text{SHMS}}}{t_{\text{auto}} n_{\text{auto}}^{\text{SHMS}} + t_{tb} n_{\text{test}}^{\text{SHMS}}}. \tag{7}$$

The cost model related to the tests needed for the first stage of certification in the laboratory of the blade is represented in equation (8) for the scenario "with SHMS":

$$\begin{aligned} C_{\text{test lab}}^{\text{SHMS}} = &\left(C_m m_{\text{blade}} + L_{tr\,wo}\left(t_{lam} + t_{em\,FBG} n_{FBG} + t_{\text{bag}} + t_{\text{mould}} + t_{\text{demould}}\right)\right. \\ &\left. + C_{FBG} n_{FBG} + L_{\text{eng}}\left(t_{tb} + t_{ev\,FBG}\right) + C_{en} t_{auto}\right) n_{\text{test}}^{\text{SHMS}} + C_{\text{test FBG sys}}, \end{aligned} \tag{8}$$

where $C_{test\,FBG\,sys}$ represents the cost of the FBG interrogation system attributed to the activity of laboratory tests calculated according to equation (9):

$$C_{\text{test FBG sys}} = C_{\text{FBG sys}} \frac{t_{tb} n_{\text{test}}^{\text{SHMS}}}{t_{\text{auto}} n_{\text{auto}}^{\text{SHMS}} + t_{tb} n_{\text{test}}^{\text{SHMS}}}. \tag{9}$$

It can be observed that the main difference between the cost models of laboratory tests in the two scenarios (equation (4) and equation (8)) is due to the fact that in the scenario "with SHMS," there is no need to apply strain gauges before testing.

3.2. Load Survey Activity. Load survey activity represents another scenario where SHMS can be exploited, and as it can be observed in Figure 6, this phase consists of two macro-activities: blade production and in-flight tests. It must be highlighted that since the component of interest in this work is represented by the helicopter blade, only its production is modelled. The first macro-activity is represented by the production of the blade (activity A1), followed by the execution of in-flight tests (activity A2). Once the blade meets the safety requirements, the latter can complete the second and last stage of certification.

The first macro-activity A1 (blade production) is represented in Figure 7, and it is quite similar to the one shown in Figure 4, but in this case, the curing cycle is already defined and the quality check consists only in performing radiography (activity A1-6). If radiography highlights some criticalities, the blade must be scrapped and a new one must be produced.

Figure 8 shows the IDEF0 diagram related to the sub-activity of in-flight tests, corresponding to the second and last stage of blade certification.

Considering the "as is" scenario, the helicopter blade must be equipped with strain gauges (activity A2-1) and the acquisition system must be mounted on the helicopter (activity A2-3). Slip ring is adopted to transfer the strain gauge signal from the rotor to the helicopter. Once the blade is mounted (activity A2-4), the helicopter is ready to perform the flight test campaign (activity A2-5). After a determined amount of time, the strain gauges applied on the blade must be removed, as they are subjected to ageing like electrical contact oxidation or debonding from the structural surface. This aspect leads the blade to be disassembled from the helicopter (activity A2-6) in order to repeat the application of the strain gauges. Data are acquired and evaluated, and once the proper safety requirements are met, the blade reaches its second and last stage of certification (activity A2-7).

Considering the scenario "with SHMS", and the related problem of receiving the OF signals from a rotating blade, the configuration of the SHMS is supposed to be similar to the one presented in [38]. Since the requirements were particularly demanding (high accelerations and vibrations), the authors in [38] required a customized interrogation

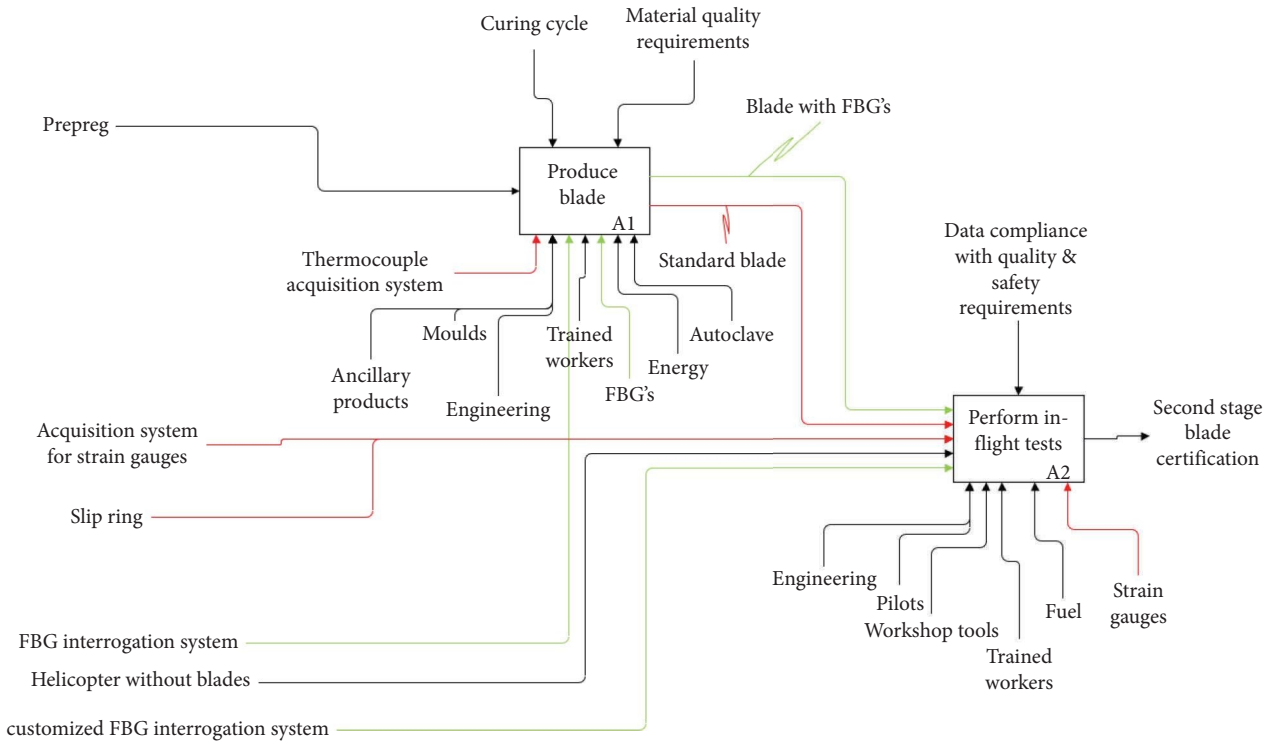

Figure 6: Load survey activity modelled with IDEF0 formalism.

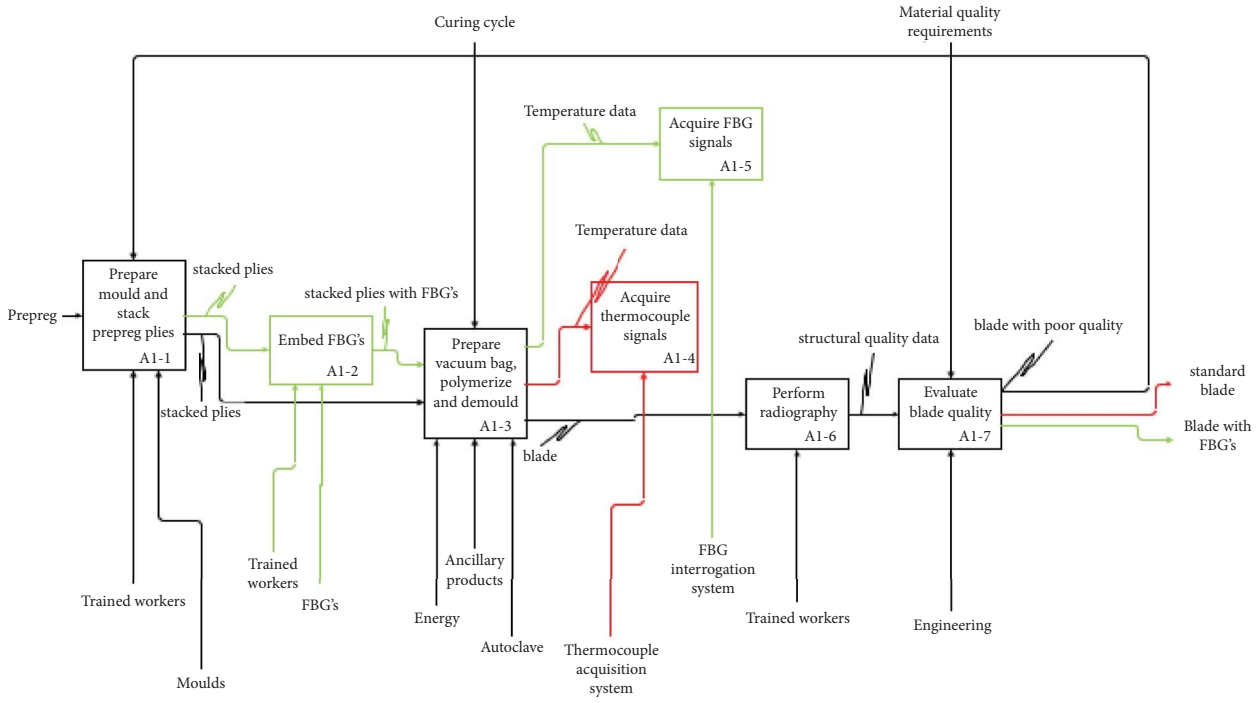

Figure 7: Activity A1, blade production modelled with IDEF0 formalism.

system housed in a dedicated beanie and mounted on the rotor hub, and the acquired strain signals were transmitted wireless to the helicopter. The interrogation system for FBG sensors must be firstly assembled on the rotor hub (activity A2-2), and the blade, already produced with FBG sensors, can be subsequently mounted on the rotor hub (activity A2-4) to perform the in-flight tests (activity A2-5). In this case, since the blade is sensorized with FBG sensors, there is no need to disassemble it, like it was done in the "as is" scenario, as such type of sensors are not

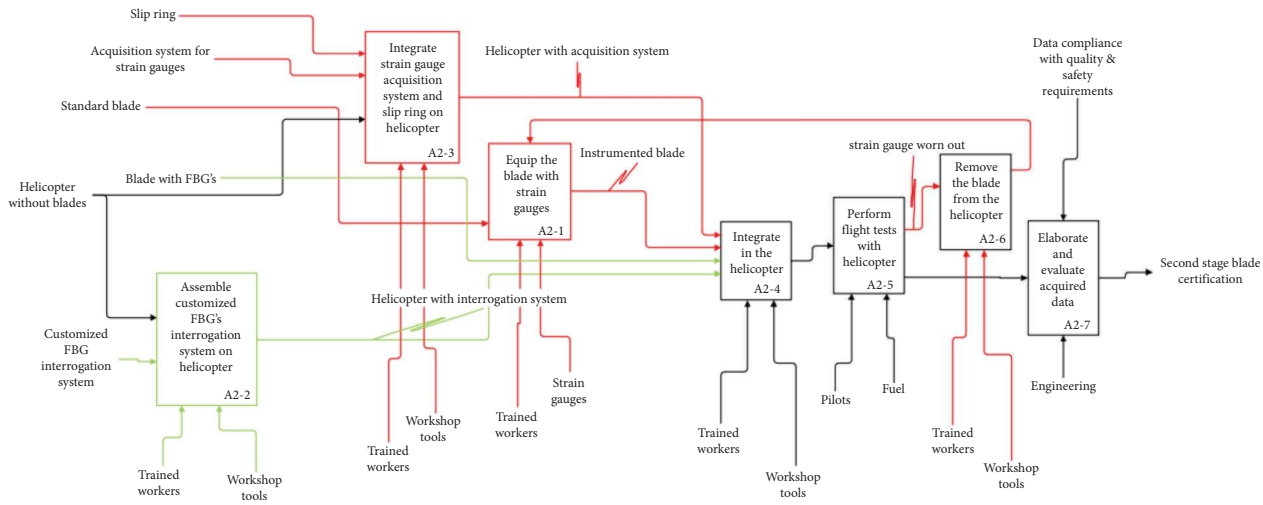

FIGURE 8: Activity A2, in flight tests modelled with IDEF0 formalism.

subjected to oxidation phenomenon and are protected inside the blade.

The total cost for the load survey activity can be obtained by summing up the costs of those two macro-activities, regardless of the type of scenario. Remarking that it expresses a differential cost between the two scenarios, the cost model related to the load survey activity is presented in equation (10):

$$C_{\text{load survey}} = n_{b\,hel} C_{\text{blade prod}} + C_{\text{flight tests}}. \tag{10}$$

The term related to the blade production $C_{\text{blade prod}}$ represents the cost to produce 1 blade and it can be calculated for the scenario "as is" using equation (11):

$$C^{\text{as is}}_{\text{blade prod}} = L_{tr\,wo} t_{em\,th} n_{th} + C_{th} n_{th} + \frac{C_{\text{acq sys}}}{n_{hel\,dep} n_{b\,hel}}. \tag{11}$$

As it can be observed, the cost consists in the depreciation of the acquisition system, that in this case is employed to monitor the curing temperature with thermocouples, and the costs related to the thermocouples. In fact, these are the only differential cost elements between the two scenarios.

Considering instead of the scenario "with SHMS," the cost to produce one helicopter blade can be described by equation (12):

$$C^{SHMS}_{blade\,prod} = L_{tr\,wo} t_{em\,FBG} n_{FBG} + C_{FBG} n_{FBG} + \frac{C_{FBG\,sys}}{n_{hel\,dep} n_{b\,hel}}. \tag{12}$$

As differential cost, both the cost of FBG sensors and their embedding are relevant; also, the depreciation of the FBG interrogation system is taken into account.

Assuming that only one helicopter is adopted by the producer company to perform the flight tests, the cost model for the "as is" scenario can be described by equation (13) and the cost model related to the scenario "with SHMS" can be described by equation (14).

$$C^{as\,is}_{flight\,tests} = n_{b\,hel}\left(L_{tr\,wo} t_g n_g + L_{tr\,wo} t_{rem\,b} + C_g n_g + L_{tr\,wo} t_{\text{int}\,b}\right) n_{equip\,gauge} + L_{tr\,wo} t_{\text{int}\,acq\,sys} + C_{acq\,sys} + C_{slip\,ring}, \tag{13}$$

$$C^{SHMS}_{flight\,tests} = n_{b\,hel}\, L_{tr\,wo} t_{\text{int}\,b} + L_{tr\,wo} t_{\text{int}\,cust\,FBG\,sys} + C_{cust\,FBG\,sys}. \tag{14}$$

It can be noticed that in the scenario "as is," represented by equation (13), the cost is dependent on the number of times and the blade is equipped with strain gauges through the variable $n_{\text{equip gauge}}$, while in the case of scenario "with SHMS," in equation (14), the sensorization of the blade with FBG sensors is done only once during the production stage.

4. Cost Model Implementation

The cost model was implemented to make the economic impact assessment. Reasonable data for the cost elements were assumed, both taken from the literature, most of them from [40], and from the experience in our laboratory. The costs are reported in Table 1.

A distinction is made between the costs of the interrogation systems. In fact, being the interrogation system used during load survey activity positioned on the helicopter tail rotor hub, it is subjected to high accelerations and vibrations, and thus, a customized device should be produced, leading to a higher cost compared to the conventional one. For this reason, a cost for the customized interrogation system $C_{\text{FBG cust sys}}$ equal to 40000 € is considered, while a cost of the conventional

Table 1: Cost values used for numerical implementation of the cost model.

Item	Cost	Source
$C_{\text{acq sys}}$	13000 €	[41]
C_{en}	10.6 €/h	[40]
C_{FBG}	90 €	Laboratory
$C_{\text{FBG cust sys}}$	40000 €	Laboratory
$C_{\text{FBG sys}}$	20000 €	[42]
C_g	1 €	[43]
C_m	181.56 €/kg	[40]
C_{th}	10 €	[44]
$C_{\text{slip ring}}$	30000 €	Laboratory
L_{eng}	42 €/h	Laboratory
$L_{\text{tr wo}}$	28 €/h	[40]

interrogation system $C_{\text{FBG sys}}$ is set to 20000 €, according to [42].

In Table 2, the time needed to perform the activities assumed in this work is reported, and in this case, all of them are assumed based on our experience in laboratory. The time for lamination was set at 24 hours, and it is justified by the manufacturing complexity represented by a helicopter blade.

In this work, it is assumed that the time to remove the blade is equal to the time to mount the blade on the rotor hub. Moreover, a number of 40 hours is considered to test one blade, considering an average between the static testing and fatigue testing. Last but not least, an assumption was required for the mass of the blade m_{blade} as this affects the costs. The mass of the blade is considered equal to 6 kg according to our knowledge in the field. In the following section 4.1 and section 4.2, the cost model is implemented for laboratory activities and for the load survey activities, respectively, finally leading to the economic impact assessment. The cost model implementation is presented by means of the sensitivity analyses over the cost elements that are affected by the application scenarios, with the purpose to enable reflecting on the effects of the variation of some key parameters.

4.1. Laboratory Activities. This section illustrates the sensitivity analyses regarding the differential costs of the laboratory activities. The results are presented by focusing, respectively, on the development of the curing cycle and on the mechanical tests for the first stage of blade certification. In Figure 9, the costs related to the development of the curing cycle for both the scenarios are expressed as function of the number of curing cycles. The sensitivity to the number of FBG sensors for the scenario "with SHMS" is investigated. The number of thermocouples n_{th} is assumed equal to 10, whereas the number of FBG sensors n_{FBG} is assumed considering 30, 20, and 10 as different options.

As it can be observed, the costs related to the scenarios "with SHMS" are always higher compared to the scenario "as is." For example, it can be observed that, for a cost of 60 k€, marked in Figure 9 with a red horizontal dashed line, the related number of curing cycles for the scenario "as is" is 26 curing cycles (point A). Considering instead the scenario "with SHMS" and the same cost of 60 k€, a number of curing

Table 2: Time needed to perform activities used for numerical implementation of the cost model.

Activity	Time needed (h)	Source
t_{auto}	8	Laboratory
t_{bag}	0.333	Laboratory
t_{demould}	0.0833	Laboratory
$t_{\text{em FBG}}$	0.083	Laboratory
$t_{\text{em th}}$	0.0167	Laboratory
$t_{\text{ev FBG}}$	0.0167	Laboratory
$t_{\text{ev }g}$	0.0167	Laboratory
$t_{\text{ev th}}$	0.0167	Laboratory
t_g	0.333	Laboratory
$t_{\text{int acq sys}}$	0.5	Laboratory
$t_{\text{int }b}$	0.125	Laboratory
$t_{\text{int cust FBG sys}}$	0.5	Laboratory
t_{lam}	24	Laboratory
t_{mould}	0.25	Laboratory
$t_{t\,b}$	40	Laboratory

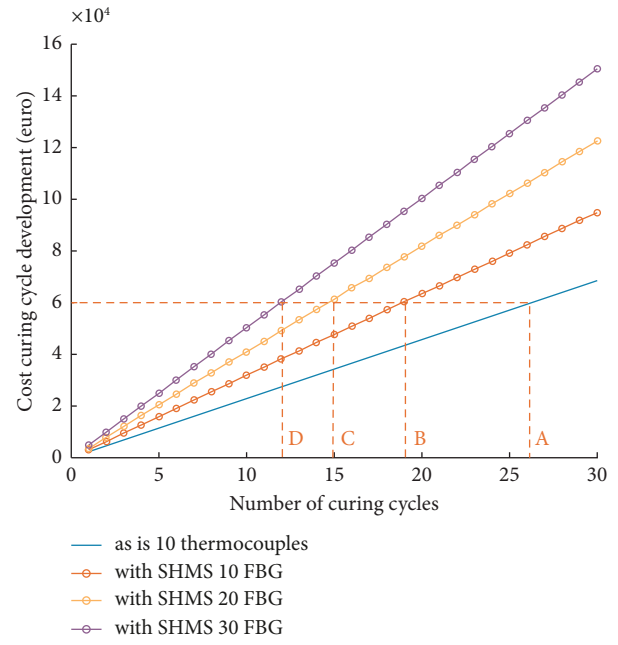

Figure 9: Differential cost of development of curing cycle function of number of curing cycles with sensitivity analysis about the number of FBG sensors. Data obtained from equations (2) and (6).

cycles equal to 19 (point B), 15 (point C) and 12 (point D) are obtained by using a number of FBG sensors equal to 10, 20, and 30, respectively. Points B, C, and D represent a target: if the increasing accuracy about temperature field due to the usage of FBG sensors allows reducing the number of curing cycles from A ("as is" scenario) below B, C, and D (scenario "with SHMS"), then the scenario "with SHMS" leads to economic benefits. It can be observed that the target values for the scenario "with SHMS", represented by the points B, C, and D, are not evenly spaced. For instance, the number of curing cycles between points C and D is equal to 3, while the number of curing cycles between C and B is equal to 4. Therefore, the target below which the scenario "with SHMS" becomes convenient and seems not to be linearly

proportional with the number of sensors integrated in the blade. However, the actual reduction in the number of curing cycles due to a higher accuracy of the temperature field using the FBG sensors may follow a different behaviour. For what concerns the laboratory tests of the blade, in Figure 10, the costs for the first stage certification tests are presented as a function of the number of tests with a sensitivity analysis related to the number of FBG sensors and to the number of strain gauges. In Figure 10(a), results are obtained for different numbers of FBG sensors n_{FBG} for the scenario "with SHMS" (10, 20, and 30) and considering for the scenario "as is," a number of strain gauges applied to the blade n_g equal to 30. In Figure 10(b), results are obtained for different numbers of strain gauges n_g for the scenario "as is" (10, 20, and 30) and considering for the scenario "with SHMS," a number of FBG sensors n_{FBG} equal to 30.

Referring to Figure 10(a), it can be observed that the scenario "with SHMS" is always more expensive than the scenario "as is." Considering a cost of 100 k€, represented by the dashed horizontal red line, a number of 22 tests should be performed for the "as is" scenario (point A). For the scenario "with SHMS using a number of FBG sensors equal to 10, 20, and 30, a number of 18 (point B), 15 (point C), and 13 (point D) tests should be, respectively, performed. Points B, C, and D represent a target: if the increasing accuracy about the strain field due to the usage of FBG sensors allows reducing the number of tests from A ("as is" scenario) below B, C, and D (scenario "with SHMS"), then the scenario "with SHMS" leads to economic benefits. Similarly to what was observed for Figure 9, it can be observed that the target values for the scenario "with SHMS", represented by the points B, C, and D, are not evenly spaced. Therefore, the target below which the scenario "with SHMS" becomes convenient and seems not to be linearly proportional with the number of sensors integrated in the blade. However, the actual reduction in the number of laboratory tests due to a higher accuracy of the strain field using the FBG sensors may follow a different behaviour. Figure 10(b) allows observing that the costs are not so much affected by the number of strain gauges applied during the testing of the blade. As a concluding remark, it can be stated that the expectation of increasing accuracy about the temperature field and strain field due to the usage of FBG sensors is effectively a key aspect in order to enable the economic benefits in the laboratory activities necessary to develop a new blade, respectively, in the curing cycle development and the mechanical laboratory tests. The sensitivity analyses herein provided show a range required for the expected increased accuracy so as to make convenient the SHMS with respect to the conventional case.

4.2. Load Survey Activity. This section illustrates the sensitivity analyses regarding the differential costs of the load survey activity. The results are presented by focusing on the number of strain gauge applications during the in-flight tests.

Before illustrating the results, some prior considerations are worth to be made.

(i) A tail rotor with a number of blades $n_{b\,hel}$ equal to 4 is considered.

(ii) The laboratory fixture corresponding to the acquisition system for thermocouples and the interrogation system to sense temperature with FBG sensors for blade production are supposed to be depreciated on a number of 150 helicopters.

(iii) A remark must be done about the nomenclature: in this work, the number of times the blade needs to be equipped with strain gauges during the in-flight tests is designated as *number of strain gauge applications during tests*, represented by the variable $n_{equip\ gauge}$. While the number of strain gauges applied to the blade is named as *number of strain gauges*, represented by the variable n_g.

(iv) The extra fuel consumption by an aircraft due to the weight increase by the SHMS is usually taken into consideration for the economic impact assessment [4, 17]. In this study, it will be neglected. The reason for that relates to the weight that the interrogation system is supposed to have. In fact, as the configuration of the SHMS considered in this work is supposed to be similar to the one presented in [38], the weight of the interrogation system is equal to 308 g. The Maximum Takeoff Weight (MTOW) of a typical helicopter like AW139 is 6400 kg [45], and thus, the difference in the fuel consumption is supposed to be negligible because the difference in weight is 0.0048%. This consideration is coupled with the relatively limited time needed to perform the in-flight tests, about 50 flight hours.

In Figure 11, the sensitivity analyses about the cost of the load survey activity as a function of the number of strain gauge applications are presented. Figure 11(a) considers the sensitivity with respect to the number of FBG sensors embedded inside the blade n_{FBG}, being the number of strain gauges applied on the blade during the in-flight tests in the "as is" $n_{equip\ gauge}$ equal to 30. Figure 11(b) instead considers the sensitivity with respect to the number of strain gauges applied on the blade during the in-flight tests in the "as is" $n_{equip\ gauge}$ against a number of FBG sensors n_{FBG} equal to 20.

Obviously, for both the sensitivity analyses (Figures 11(a) and 11(b)), the cost related to the scenario "with SHMS" is not dependent on the number of strain gauge applications, as that operation is performed only in the scenario "as is." Said this, it is interesting to observe that a break-even point in the number of strain gauge applications during the load survey activity exists, and it is marked with letters A, B, and C for Figure 11(a) and for Figure 11(b). It can also be observed that it is highly dependent on both the number of FBG sensors and the number of strain gauges applied on the blade at each strain gauge application. Break-even point represents a target: the number of strain gauge application during the load survey activity over which one of the two scenarios starts becoming more expensive (then, less convenient) than the other one. Consider for example the break-even point marked with letter A in Figure 11(b) for a number of strain gauges equal to 30. It can be seen that for a number of about 9 strain gauge applications, the

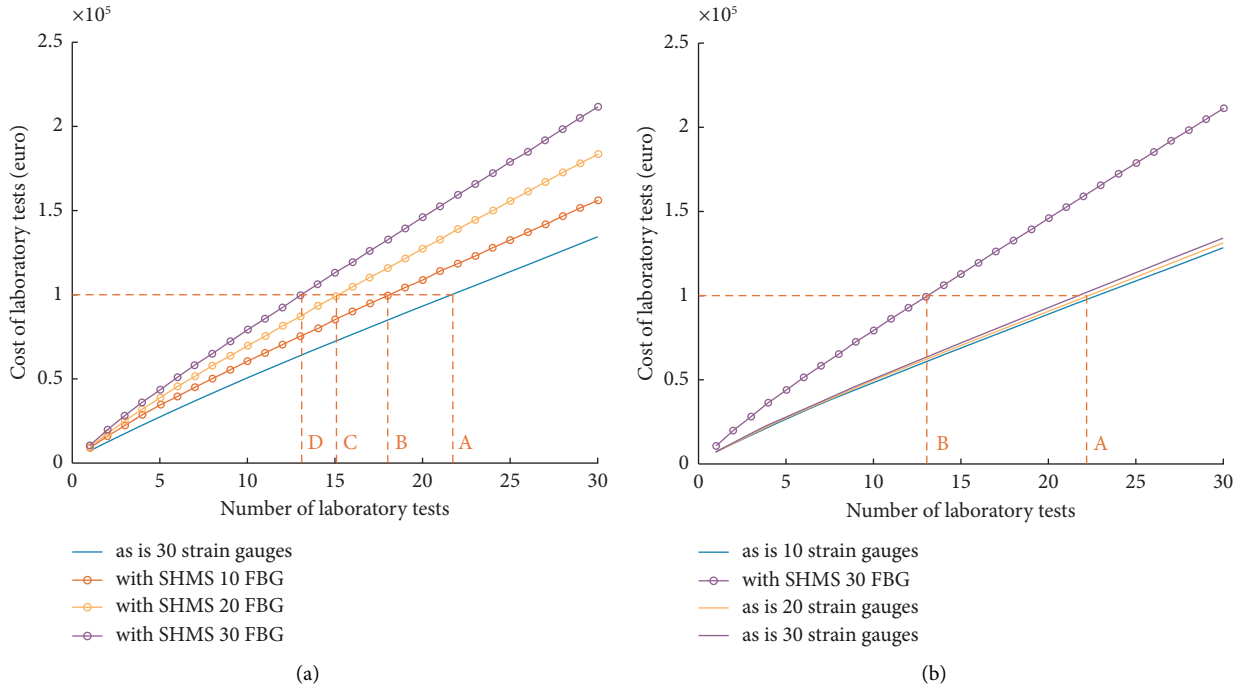

FIGURE 10: Differential cost of mechanical laboratory tests needed for the first stage of blade certification with sensitivity analysis about (a) number of FBG sensors and (b) number of strain gauges. Data obtained from equations (4) and (8).

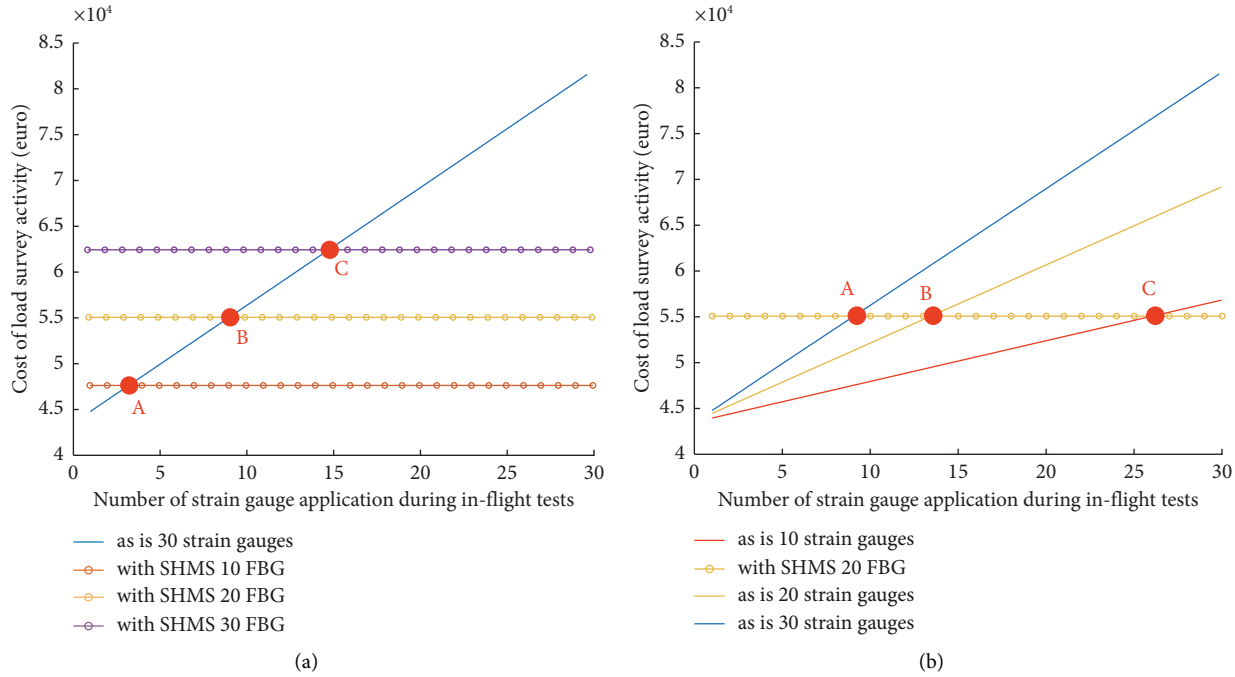

FIGURE 11: Sensitivity analysis related to differential cost of load survey activity for "as is" scenario and scenario "with SHMS" for (a) different number of FBG sensors and (b) different number of strain gauges. Data obtained from equation (10).

scenario "as is" starts becoming more expensive (then less convenient) than the scenario "with SHMS." Looking at Figure 11(a), it is interesting to observe that for a number of FBG sensors equal to 10, the scenario "with SHMS" starts becoming more convenient after a number of 3 strain gauge applications on the blade, in correspondence of the point A. By increasing the number of FBG sensors to 20 and 30, the scenario "with SHMS" starts providing economic benefits after a number of 9 and 15 strain gauge applications, corresponding to the letters B and C, respectively.

It must be remarked that in the presented cost models, the potential failure of some FBG sensors, as well as thermocouples and strain gauges, are not considered. Indeed, such cost models provide some target thresholds, across which one of the two scenarios becomes more convenient than the other one. The possible failure of a sensor would impact the quality of the strain/temperature field, affecting the number of curing cycles, laboratory tests, and/or the number of strain gauge applications during the load survey activity. Some experiments should be performed to quantify the actual reduction in the number of curing cycles, laboratory tests, and strain gauge applications; such experimental results will also depend on the probability of the sensors to fail during such processes.

5. Conclusions

A cost model for the development of composite sensorized tail rotor blades is presented in this work, highlighting some of the benefits that SHMS may provide. SHMS are supposed to be useful during the development phase of a new composite blade, especially by monitoring the temperature field for the development of the curing cycle, and by monitoring the mechanical strain field during the tests for the first stage blade certification. Another application that is investigated is related to the load survey activity. Indeed, the tests that the helicopter's blade must perform during the load survey may be supported by SHMS without the need to apply the strain gauges multiple times.

It was found that if the number of curing cycles are reduced from 26 in the scenario "as is" below the target of 19 using 10 FBG sensors, then an economic benefit is achieved exploiting the SHMS. It was also found that the target value changes with the number of FBG sensors embedded in the blade. The results about the application of the SHMS on the first stage certification tests show that an economic benefit can be achieved if the number of tests performed on the blade reduces from 22, in the scenario "as is," below the target of 18 using 10 FBG sensors. Such target seems to depend on the number of FBG sensors embedded in the blade, while a low sensitivity to the number of strain gauges applied on the blade in the scenario "as is" was found. Results about the load survey activity highlighted an interesting aspect, which is represented by the presence of break-even points: if the number of strain gauge applications in a blade having 30 strain gauges exceeds 4, then the scenario "with SHMS" with 10 FBG's starts providing economic benefits. The break-even points are deeply influenced by the number of the FBG sensors embedded in the blade and by the number of strain gauges applied on the blade.

Future works will be needed to quantify experimentally the potential reduction in the number of curing cycles, as well as the potential reduction in the number of tested blades in the presence of an SHMS: these will also provide the information about the potential sensors faults and how this impacts the potential saving obtained using the FBG sensors. Although the cost model is developed on a case study of a helicopter tail rotor blade, the same model can be applied to main rotor blades using different values for the variables: for instance using a different blade mass and a different lamination time. The cost models can also be adapted to other composite structural elements different from a blade: in this case, some changes to the cost model must be done, neglecting the cost of the slip ring for the scenario "as is" and the cost of the customized interrogation system for the scenario "with SHMS."

Nomenclature

$\ldots^{\text{as is}}$:	Cost element related to the "as is" scenario
$C_{\text{acq sys}}$:	Cost of one acquisition system
C_{en}:	Cost per unit of time of energy for autoclave curing cycle
C_{FBG}:	Cost of one FBG sensor
$C_{\text{FBG cust sys}}$:	Cost of one FBG customized interrogation system
$C_{\text{FBG sys}}$:	Cost of one FBG interrogation system
C_g:	Cost of one strain gauge
C_m:	Cost of prepreg material
$C_{\text{slip ring}}$:	Cost of one slip ring
C_{th}:	Cost of one thermocouple
L_{eng}:	Labour rate per engineer hour
$L_{\text{tr wo}}$:	Labour rate per trained worker hour
m_{blade}:	Mass of the blade
n_{auto}:	Number of autoclave curing cycles
n_b:	Number of blades produced
$n_{b\,hel}$:	Number of blades per helicopter (is equal to4 in our case)
$n_{\text{equip gauge}}$:	Number of times the blades need to be equipped with strain gauges during load survey activity
n_{FBG}:	Number of FBG sensors to use in one blade
n_g:	Number of strain gauges applied to one blade
$n_{\text{hel dep}}$:	Number of helicopters over which acquisition systems are depreciated
n_{test}:	Number of blade tested in laboratory
n_{th}:	Number of thermocouples embedded or applied to monitor temperature during curing cycle
$\ldots^{\text{SHMS}}$:	Cost element attributed to the scenario "with SHMS"
t_{auto}:	Time to polymerize one blade in autoclave
t_{bag}:	Time to prepare vacuum bag
t_{demould}:	Time to remove blade from mould
$t_{\text{em FBG}}$:	Time to embed one FBG sensor
$t_{\text{em th}}$:	Time to embed one thermocouple or to apply one thermocouple on mould
$t_{\text{ev FBG}}$:	Time to evaluate FBG data quality
$t_{\text{ev}\,g}$:	Time to evaluate strain gauge data quality obtained during blade testing
$t_{\text{ev th}}$:	Time to evaluate thermocouple data quality
t_g:	Time to apply one strain gauge
$t_{\text{int acq sys}}$:	Time to integrate strain gauge acquisition system and slip ring in the helicopter
$t_{\text{int}\,b}$:	Time to integrate one blade in the helicopter
$t_{\text{int cust FBG sys}}$:	Time to integrate customized FBG acquision system in the helicopter

t_{lam}: Time for lamination of the blade
t_{mould}: Time to prepare the mould
$t_{\text{rem}\,b}$: Time to remove one blade from the helicopter
$t_{t\,b}$: Time to test one blade in laboratory.

Data Availability

Data are available on request.

Conflicts of Interest

The authors declare that there are no conflicts of interest regarding the publication of this article.

Acknowledgments

Open access publishing was facilitated by Politecnico di Milano, as part of the Wiley-CRUI-CARE agreement.

References

[1] J. Van den Bergh, P. De Bruecker, J. Beliën, and J. Peeters, "Aircraft maintenance operations: state of the art," *HUB Research Paper 2013/09*, 2013.

[2] P. Y. Cho, *Optimal Scheduling of Fighter Aircraft Maintenance*, Doctoral dissertation, Massachusetts Institute of Technology, 2011.

[3] A. Steiner, "A heuristic method for aircraft maintenance scheduling under various constraints," in *Proceedings of the 6th Swiss Transport Research Conference*, Ancona, Italy, March 2006.

[4] T. Dong and N. H. Kim, "Cost-effectiveness of structural health monitoring in fuselage maintenance of the civil aviation industry," *Aerospace*, vol. 5, no. 3, p. 87, 2018.

[5] L. Fitzwater, C. Davis, T. Torng, and J. Poblete, "Cost/benefit analysis for intergration of non-deterministic analysis and in-situ monitoring for structural integrity," in *Proceedings of the 52nd AIAA/ASME/ASCE/AHS/ASC Structures, Structural Dynamics and Materials Conference 19th AIAA/ASME/AHS Adaptive Structures Conference 13t*, September 2003.

[6] X. Chen, H. Ren, and C. Bil, "Inspection intervals optimization for aircraft composite structures considering dent damage," *Journal of Aircraft*, vol. 51, no. 1, pp. 303–309, 2014.

[7] S. Gholizadeh, "A review of non-destructive testing methods of composite materials," *Procedia Structural Integrity*, vol. 1, pp. 50–57, 2016.

[8] K. T. Tan, N. Watanabe, and Y. Iwahori, "X-ray radiography and micro-computed tomography examination of damage characteristics in stitched composites subjected to impact loading," *Composites Part B: Engineering*, vol. 42, no. 4, pp. 874–884, 2011.

[9] U. Polimeno and M. Meo, "Detecting barely visible impact damage detection on aircraft composites structures," *Composite Structures*, vol. 91, no. 4, pp. 398–402, 2009.

[10] V. Giurgiutiu, "Structural health monitoring of aerospace composites," 2015.

[11] L. Pollock, A. K. Abdelwahab, J. Murray, and G. Wild, "The need for aerospace structural health monitoring: a review of aircraft fatigue accidents," 2021.

[12] A. Güemes, A. Fernandez-Lopez, A. R. Pozo, and J. Sierra-Pérez, "Structural health monitoring for advanced composite structures: a review," *Journal of Composites Science*, vol. 4, no. 1, p. 13, 2020.

[13] J. Alvarez-Montoya, M. Torres-Arredondo, and J. Sierra-Pérez, "Gaussian process modeling for damage detection in composite aerospace structures by using discrete strain measurements," in *Proceedings of the 7th Asia-Pacific Workshop on Structural Health Monitoring*, pp. 710–718, June 2018.

[14] R. Di Sante, "Fibre optic sensors for structural health monitoring of aircraft composite structures: recent advances and applications," *Sensors*, vol. 15, no. 8, pp. 18666–18713, 2015.

[15] A. Airoldi, P. Ballarin, S. Di Mauro et al., "Development of an additive manufactured fitting sensorized with optical fibres for load recognition," in *AIAA Scitech 2023 Forum*, 2023.

[16] G. Sala, L. Di Landro, A. Airoldi, and P. Bettini, "Fibre optics health monitoring for aeronautical applications," *Meccanica*, vol. 50, no. 10, pp. 2547–2567, 2015.

[17] K. D. Büchter, C. Sebastia Saez, and D. Steinweg, "Modeling of an aircraft structural health monitoring sensor network for operational impact assessment," *Structural Health Monitoring*, vol. 21, no. 1, pp. 208–224, 2022.

[18] D. M. Steinweg, M. Hornung, and W. Bauhaus Luftfahrt eV, *Methods Evaluating the Impact of Structural Health Monitoring on Aircraft Lifecycle Costs*, 2019.

[19] S. Pattabhiraman, C. Gogu, N. H. Kim, R. T. Haftka, and C. Bes, "Skipping unnecessary structural airframe maintenance using an on-board structural health monitoring system," *Proceedings of the Institution of Mechanical Engineers - Part O: Journal of Risk and Reliability*, vol. 226, no. 5, pp. 549–560, 2012.

[20] V. Cusati, S. Corcione, and V. Memmolo, "Impact of structural health monitoring on aircraft operating costs by multidisciplinary analysis," *Sensors*, vol. 21, no. 20, p. 6938, 2021.

[21] V. Cusati, S. Corcione, and V. Memmolo, "Potential benefit of structural health monitoring system on civil jet aircraft," *Sensors*, vol. 22, no. 19, p. 7316, 2022.

[22] V. Mugnaini, L. Zanotti Fragonara, and M. Civera, "A machine learning approach for automatic operational modal analysis," *Mechanical Systems and Signal Processing*, vol. 170, Article ID 108813, 2022.

[23] L. Sibille, M. Civera, L. Zanotti Fragonara, and R. Ceravolo, "Automated operational modal analysis of a helicopter blade with a density-based cluster algorithm," *AIAA Journal*, vol. 61, no. 3, pp. 1411–1427, 2023.

[24] S. Weber, T. Kissinger, E. Chehura et al., "Application of fibre optic sensing systems to measure rotor blade structural dynamics," *Mechanical Systems and Signal Processing*, vol. 158, Article ID 107758, 2021.

[25] Iso, *Petroleum and Natural Gas Industries—Life-Cycle Costing—Part 1: Methodology*.

[26] Iso, *Petroleum and Natural Gas Industries—Life-Cycle Costing—Part 2: Guidance on Application of Methodology and Calculation Methods*.

[27] Iso, *Petroleum and Natural Gas Industries—Life-Cycle Costing—Part 3: Implementation Guidelines*.

[28] E. Korpi and T. Ala-Risku, "Life cycle costing: a review of published case studies," *Managerial Auditing Journal*, vol. 23, no. 3, pp. 240–261, 2008.

[29] D. Rigamonti and P. Bettini, "Enabling FO-based HUMS applications through an innovative integration technique: application to a rotor blade mockup," in *European Workshop on Structural Health Monitoring*, 2022.

[30] G. Sciamé, D. Rigamonti, P. Bettini, P. Tagliabue, and G. Sala, "An integrated fiber optic based SHM system for structural

composite components: application to a racing motorbike fork," in *European Workshop on Structural Health Monitoring*, pp. 933–942, 2022.

[31] F. Badurdeen, M. Shuaib, and J. P. Liyanage, "Risk modeling and analysis for sustainable asset management," in *Engineering Asset Management and Infrastructure Sustainability: Proceedings of the 5th World Congress on Engineering Asset Management (WCEAM 2010)*, pp. 61–75, 2012.

[32] M. Z. Ouertani, A. K. Parlikad, and D. C. McFarlane, "Towards an approach to select an asset information management strategy," *International Journal of Computer Science and Applications*, vol. 5, no. 3b, pp. 25–44, 2008.

[33] D. Kiritsis, V. K. Nguyen, and J. Stark, "How closed-loop PLM improves Knowledge Management over the complete product lifecycle and enables the factory of the future," *International Journal of Product Lifecycle Management*, vol. 3, no. 1, pp. 54–77, 2008.

[34] Z. Liu, X. Zheng, L. Gao, L. Yan, G. Song, and S. Zhang, "Comparative study on the effect of cure parameters on residual deformation for thermoset composite laminates," *Journal of Composite Materials*, vol. 55, no. 19, pp. 2591–2604, 2021.

[35] Z. S. Guo, "Strain and temperature monitoring of asymmetric composite laminate using FBG hybrid sensors," *Structural Health Monitoring*, vol. 6, no. 3, pp. 191–197, 2007.

[36] S. Ghiasvand, A. Airoldi, P. Bettini, and C. Mirani, "Analysis of residual stresses and interface damage propagation in hybrid composite/metallic elements monitored through optical fiber sensors," *Aerospace Science and Technology*, vol. 129, Article ID 107373, 2022.

[37] J. Chen, J. Wang, X. Li, L. Sun, S. Li, and A. Ding, "Monitoring of temperature and cure-induced strain gradient in laminated composite plate with FBG sensors," *Composite Structures*, vol. 242, Article ID 112168, 2020.

[38] L. M. Bottasso, G. Sala, P. Bettini et al., "Rugged fiber optics monitoring system for helicopter rotor blades," in *44th European Rotorcraft Forum (ERF 2018)*, pp. 965–980, Curran Associates, 2018.

[39] M. C. Emmons, S. Karnani, S. Trono, K. P. Mohanchandra, W. L. Richards, and G. P. Carman, "Strain measurement validation of embedded fiber Bragg gratings," *International Journal of Optomechatronics*, vol. 4, no. 1, pp. 22–33, 2010.

[40] L. Morse, L. Cartabia, and V. Mallardo, "Reliability-based bottom-up manufacturing cost optimisation for composite aircraft structures," *Structural and Multidisciplinary Optimization*, vol. 65, no. 5, p. 159, 2022.

[41] https://b2bstore.hbm.com/myHBM/app/displayApp/(cpgnum=1%26layout=7.01-16_153_6_9_70_34_65_73_134_6%26uiarea=6%26citem=CC58514E6AD90F12E1000000AC1099340017A47744441EE1B2B08ED8335B1888%26carea=CC58514E6AD90F12E1000000AC109934%26rdb=0%26cpgsize=0)/.do?rf=y.

[42] https://b2bstore.hbm.com/myHBM/app/displayApp/(cpgnum=1%26layout=7.01-16_153_6_9_70_34_65_73_134_6%26uiarea=6%26citem=319DCC4F1E60564AE1000000AC109A0CA01D4895C9E81EE79BC34A9F7F62510B%26carea=319DCC4F1E60564AE1000000AC109A0C%26xcm=hbm_b2boccasionalcrm%26rdb=0%26cpgsize=0)/.do?rf=y.

[43] https://www.amazon.com/dp/B08SLP6W18/ref%3Dsspa_dk_detail_2?pd_rd_i%3DB08SLP6W18%26pd_rd_w%3DPcrZM%26content-id%3Damzn1%2Esym%2E0d1092dc-81bb-493f-8769-d5c802257e94%26pf_rd_p%3D0d1092dc-81bb-493f-8769-d5c802257e94%26pf_rd_r%3DNZ4Q1Z7XPQ2RPBP6CS1E%26pd_rd_wg%3DZGxkA%26pd_rd_r%3D5e7c4249-2c36-4c2f-a444-7dbbad428b58%26s%3Dindustrial%26sp_csd%3Dd2lkZ2V0TmFtZT1zcF9kZXRhaWwy%26th%3D1.

[44] https://www.ersa-shop.de/de/product_info.php?info=p1912_themoelement-k-type.html&gad=1&gclid=EAIaIQobChMIyZ3T4q-DgAMVqItoCR2UhACiEAQYDSABEgL8D_D_BwE.

[45] https://it.wikipedia.org/wiki/AgustaWestland_AW139.